Magneto-electronic properties and spin-resolved I–V curves of a Co/GeSe heterojunction diode: an ab initio study

Leonardo Makinistian & Eduardo A. Albanesi

Applied Physics A
Materials Science & Processing

ISSN 0947-8396
Volume 111
Number 3

Appl. Phys. A (2013) 111:923-927
DOI 10.1007/s00339-012-7315-6

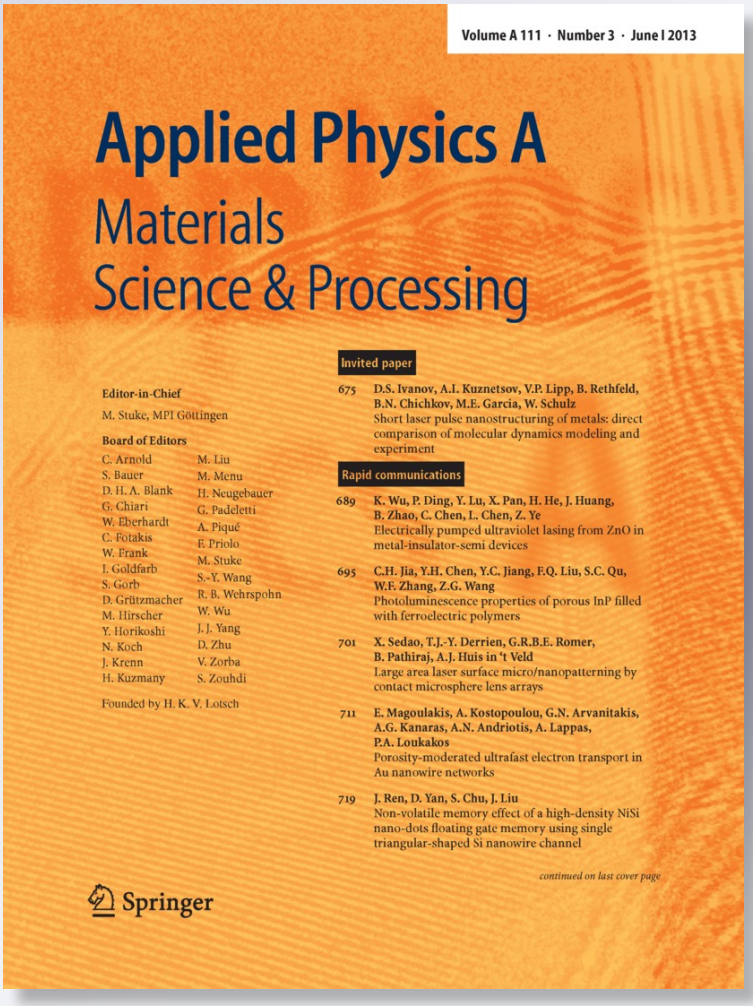

Springer

Appl Phys A (2013) 111:923–927
DOI 10.1007/s00339-012-7315-6

Applied Physics A
Materials Science & Processing

Magneto-electronic properties and spin-resolved I–V curves of a Co/GeSe heterojunction diode: an ab initio study

Leonardo Makinistian · Eduardo A. Albanesi

Received: 20 June 2012 / Accepted: 4 October 2012 / Published online: 18 October 2012

Abstract We present ab initio calculations of magnetoelectronic and transport properties of the interface of hcp Cobalt (001) and the intrinsic narrow-gap semiconductor germanium selenide (GeSe). Using a norm-conserving pseudopotentials scheme within DFT, we first model the interface with a supercell approach and focus on the spin-resolved densities of states and the magnetic moment (spin and orbital components) at the different atomic layers that form the device. We also report a series of cuts (perpendicular to the plane of the heterojunction) of the electronic and spin densities showing a slight magnetization of the first layers of the semiconductor. Finally, we model the device with a different scheme: using semiinfinite electrodes connected to the heterojunction. These latter calculations are based upon a nonequilibrium Green's function approach that allows us to explore the spin-resolved electronic transport under a bias voltage (spin-resolved I–V curves), revealing features of potential applicability in spintronics.

1 Introduction

Since the late 1980s, with the discovery of the giant magnetoresistance (GMR) in metallic multilayers (e.g., $[Fe/Cr]_n$, o $[Co/Cu]_n$) [1], there has been an ever increasing interest in magnetic phenomena of heterostructures such as superlattices [2, 3], double-barrier heterojunctions [4], single and double magnetic tunnel junctions (TMJ [5] and DMTJ [6]), or single-molecule junctions [7]. All of these material systems are composed of several interfaces, thus a thorough comprehension of electronic, magnetic, and transport properties of them is crucial in the realm of spintronics [8]. The injection of currents polarized in spin (either from a ferromagnet or a magnetic semiconductor) into a non-magnetic semiconductor represents a key to the integration of the emerging spintronics with the well-established semiconductor electronics technology. The use of semiconductors presents the advantages of (a) the existence of a band gap that is usually tunable in a family of ternary compounds; (b) their optical properties, that allow for optoelectronic applications; and (c) the possibility of controlling carrier concentrations with doping [8, 9]. In spite of the latter, there has been a certain interest in the use of *intrinsic* semiconductors for the development of devices such as double-heterostructure midinfrared PIN (p-type/intrinsic/n-type) lasers [10], and heterojunction diodes [11, 12]. Furthermore, it has been experimentally proven for spin-diodes that the use of an intrinsic semiconductor provides better tunability upon magnetic field application, and higher magnetoresistances than those obtained using n- or p-doped semiconductors [13].

Motivated for those results, in this work, we model the heterojunction of (001) hcp cobalt with a narrow-gap intrinsic (i.e., nondoped) semiconductor: GeSe. Similarly to ab initio calculations of interfaces of hcp Co with diamond [14], and with alumina [15], here the ground-state magnetoelectronic properties of the Co/GeSe interface are investigated with a supercell within DFT. However, we fur-

L. Makinistian (✉) · E.A. Albanesi
INTEC-CONICET, Güemes 3450, 3000 Santa Fe, Argentina
e-mail: lmakinistian@santafe-conicet.gov.ar
Fax: +54-342-4550944

E.A. Albanesi
e-mail: eaa@santafe-conicet.gov.ar
Fax: +54-342-4550944

L. Makinistian · E.A. Albanesi
Facultad de Ingeniería, Universidad Nacional de Entre Ríos, 3101 Oro Verde (ER), Argentina

ther use a nonequilibrium Green's functions (NEGF) approach based on a semiinfinite electrodes model to assess spin-resolved transmission, conductance, and current under a bias voltage. We discuss the spin-polarized current injection from the ferromagnet to the semiconductor and the rectifying features of the heterojunction.

2 Computational details

All calculations were performed with the software suite OpenMX [16], using fully relativistic norm-conserving pseudopotentials, and pseudoatomic orbitals (PAOs) for the expansion of the wave function, both contributed by Ozaki and Kino [17, 18]. The PAO basis functions were specified by Co5.5-s2p2d1, Ge5.0-s2p2d1, and Se5.0-s2p2d1, where, e.g., Co is the atomic symbol, 5.5 is the cutoff radius (Bohr) according to the confinement scheme utilized [17, 18], and s2p2d1 means the employment of two primitive orbitals for each s and p orbital and one for the d orbital. We used the Perdew–Burke–Ernzerhof [19–21] Generalized Gradient Approximation for the exchange and correlation, plus a Coulomb potential (GGA + U, e.g., [22]), with an effective U of $U_{\text{eff}} = 0.789$ eV. The latter is needed for the correct description of the d-bands of cobalt according to Shick and Mryasov [23].

We used a supercell with 5 layers of Co and 8 atomic layers of GeSe. This semiconductor's layers are not strictly planar but present a slight corrugation, and form bilayers perpendicular to the longest axis of the crystal, with covalent bonds within each bilayer and weak van der Waals bonding between them, Fig. 1a [24]. This structure strongly suggests that a free (100) surface of GeSe will present dangling bonds only if the bulk is cut through the middle of a bilayer, e.g., between l_6 and l_7 in Fig. 1a. On the contrary, a surface including an integer number of bilayers is to be expected to show "self-saturation," i.e., the absence of dangling bonds and so no need of adding hydrogens to passivate it. We tested and confirmed this ideas with calculations of both types of GeSe surfaces: upon this auxiliary calculations, we found the effect of adding hydrogen atoms neglectable, and so we did not include them in our calculations of the interface with cobalt. We did include a vacuum slab of ∼12 Å in the supercell to avoid coupling due to the periodic conditions (e.g., [14]), finally yielding a supercell of: 42.5834 × 4.3782 × 7.6227 Å with a total of 62 atoms (30 Co, 16 Ge, and 16 Se). The acceptable lattice mismatches of 0.8 % and 1.3 % for the y and z axes were necessary to build the supercell (the plane of the interface is perpendicular to the x axis); see Figs. 1a and 2c–d.

For the discretization of real space, we used a 540 × 56 × 98 points mesh (cutoff energy of 450 Ry) and the four atomic layers closer to the interface plane were left to relax (leaving all the rest with their atomic positions fixed) to a maximum force of $\sim 10^{-2}$ Ha/Bohr), using a 1 × 5 × 5 Monkhorst [25] mesh. Electronic densities and densities of states (DOS) were calculated with a 1 × 2 × 2 mesh for the SCF and a further refinement to 1 × 5 × 5, and these same mesh densities were adopted for the NEGF calculations. For these latter, however, the interface is modeled with semi-infinite electrodes (e.g., [26]) in terms of three regions: L_0 and R_0 for left and right electrodes (that are replicated ad infinitum semiperiodically) and C_0; see Fig. 1b (and [16] for a thorough discussion). A temperature of 600 K ($kT \sim 50$ meV) was used in the Fermi–Dirac distribution and a convergence of the total magnetic moment was accomplished within a ∼10 % of the one obtained with the supercell model. While the supercell calculations included the spin-orbit coupling, the NEGF approach described only collinear magnetism, i.e., spin-orbit is not included in the electronic transport calculations.

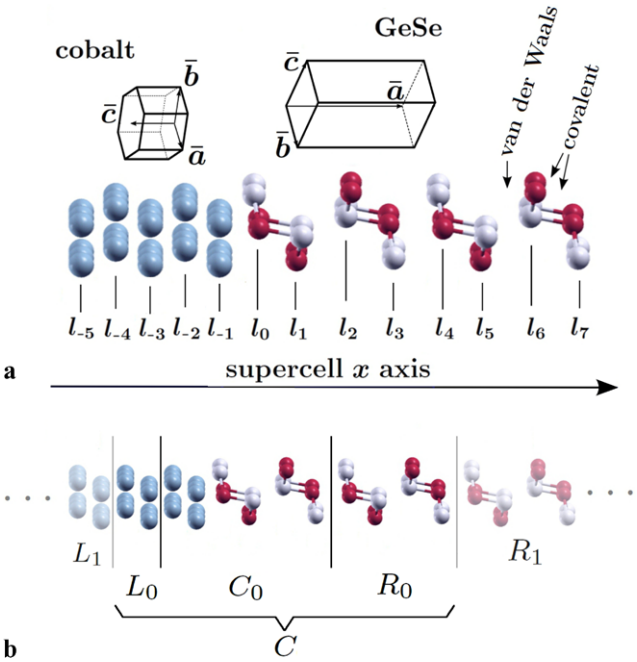

Fig. 1 (**a**) Supercell model of the interface for ground-state properties; layers l_{-5}–l_{-1}: Co, layers l_0–l_7: GeSe. The hexagonal and orthorhombic unit cells of cobalt and GeSe are displayed to show their relative orientation: the longest primitive vector of Co, $\bar{c}$ (cobalt's [001] direction), and that of GeSe, $\bar{a}$ (germanium selenide's [100] direction), are parallel to each other and to the x axis of the supercell (also see Figs. 2c–d below). (**b**) Semiinfinite electrodes model of the same interface for NEGF assessment of I–V_b curves. All the structural information is within region C: regions $L(R)_j$ with $j = 1, 2, \ldots$ are identical to $L(R)_0$

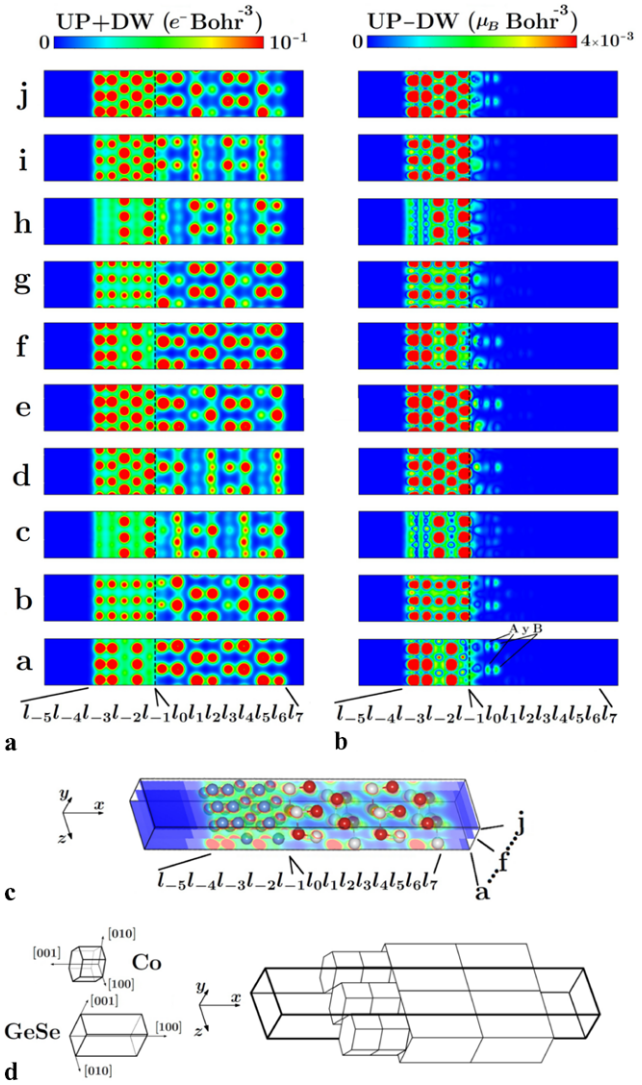

Fig. 2 (**a**) Ten successive cuts (a...f...j, parallel to xz plane of the supercell) of the electronic charge (UP + DW) and (**b**) spin moment (UP–DW) of the interface. (**c**) Unit cell illustrating the direction of the cuts. (**d**) The supercell and some unit cells of cobalt and GeSe showing the correspondence of supercell's axes (x, y and z) and the two materials (Co and GeSe) crystallographic directions: $x \parallel [001]_{\text{Co}} \parallel [100]_{\text{GeSe}}$, $y \parallel [210]_{\text{Co}} \parallel [001]_{\text{GeSe}}$, and $z \parallel [100]_{\text{Co}} \parallel [010]_{\text{GeSe}}$

3 Discussion of results

3.1 Electron and spin densities, and DOS

In order to have a combined image of the crystallographic, electronic, and magnetic structures of the interface in real space, in Figs. 2a–b, we show cuts (at 10 equidistant planes: a...f...j, parallel to the xz plane of the supercell) of the electronic charge (UP + DW) and the spin (UP–DW) densities at both sides of the interface, indicated by the dashed lines. The bilayered structure [24] of GeSe is clear, with covalent bonds within the bilayers (l_0l_1), (l_2l_3), (l_4l_5), and (l_6l_7) and van der Waals bonds between them. The metallic nature of cobalt is also clear from the absence of dark areas on its side. The bond at the interface is of metallic/covalent nature, and an analysis of Fig. 3 indicates that it is mostly due to electronic charge yielded by Se atoms of l_0 with a minor contribution of the Ge atoms. The right column of Fig. 2 shows that spin polarization on the cobalt side is maximum at and near the atomic sites but nonneglectable in the interstitial space, while in contrast (as expected) most part of the semiconductor is nonmagnetic. However, there is some magnetization penetrating into the two GeSe layers near the interface (see Fig. 3b). The Se atoms present a clearly asymmetrical distribution of magnetic moment around them, see lobes A y B in cut a, almost specular with respect to a plane parallel to yz and passing through the Se atomic sites. Here, the key point from the calculated densities is that (a) magnetization of GeSe only exists in the first atomic layers closer to the interface and its magnitude is much lower than that of Co (see below for quantification), and (b) that its sign is the same as that of Co, i.e., the two materials couple ferromagnetically.

In Fig. 3a, spin and orbital-resolved DOS are presented for selected layers: l_{-1} and l_0 (closest to the interface), and l_{-3} and l_4 (away from the interface, bulk-like). Figure 3b shows the absolute magnetic moment per layer (resolved for Ge and Se atoms): the spin and orbital magnetic moments at l_{-3} are $1.72\mu_B$ and $0.13\mu_B$, respectively (experimental values [23]: 1.52 and $0.14\mu_B$, respectively), while at the Co side of the interface, l_{-1}, they are slightly different: $1.68\mu_B$ and $0.14\mu_B$. The moments are strongly quenched on the GeSe side, with one of only $\sim 0.1\mu_B$ remaining (almost of pure spin origin: orbital moment vanishes). The inset of Fig. 3b shows the relative spin polarization, P_{DOS}, of DOSs at E_F for the layers of highest interest: There is an increase of $\sim$5 % for P of Co at the interface, before it drastically drops to ~ -50 % (Ge) and ~ -35 % (Se) at l_0, and ~ -37 % (Ge) and ~ -22 % (Se) at l_1, and 0 % for $l_{i>1}$. An analysis of the integral of the DOSs comparing the most bulk-like (l_{-3} and l_4) layers against the ones at the interface (l_{-1} and l_0) allows to determine that while total charge of Co atoms remains almost the same, there is a substantial lost of charge from GeSe atomic spheres to the interstitial space ($\sim$20 % for Se and $\sim$6 % for Ge). DOSs also show how the contact with the ferromagnet closes the gap of GeSe at the interface, which is occupied by s and p states asymmetrically for majority and minority electrons: In l_0, at E_F, s and p electrons have similar contributions for Ge atoms, while s contribution is almost neglectable for Se atoms.

3.2 Electronic transport

Figures 4a–c show the spin dependent transmission coefficients, $T_\sigma(E)$, for the interface under three different bias voltages. The cobalt electrode is taken as reference (with

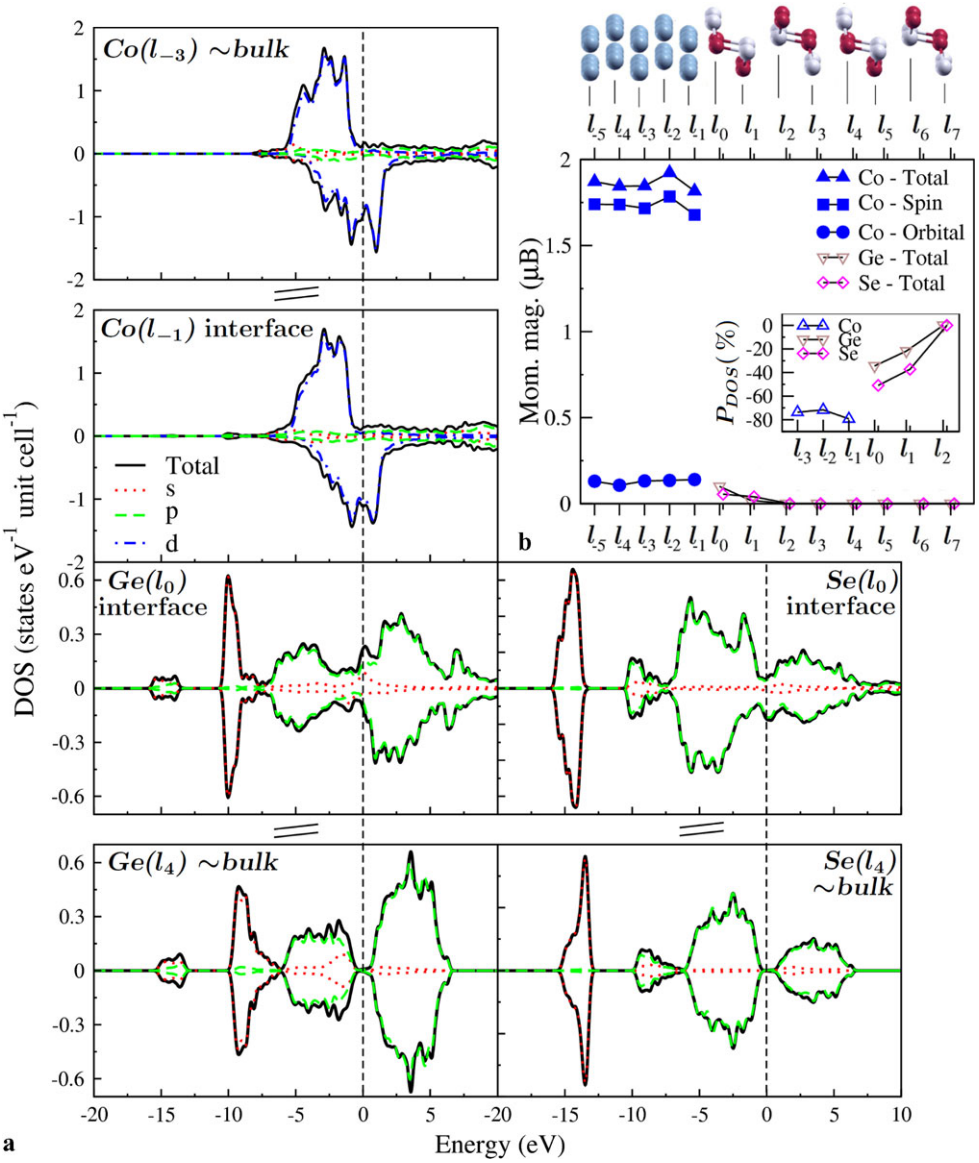

Fig. 3 (**a**) Orbital and spin-resolved DOS for selected layers of the Co/GeSe interface. (**b**) Spin, orbital, and total magnetic moment per layer, and spin polarization, $P_{\mathrm{DOS}}(\%) = \frac{N^{\uparrow}(E_F) - N^{\downarrow}(E_F)}{N^{\uparrow}(E_F) + N^{\downarrow}(E_F)} \times 100$, at the atomic layers of highest interest (see *inset*)

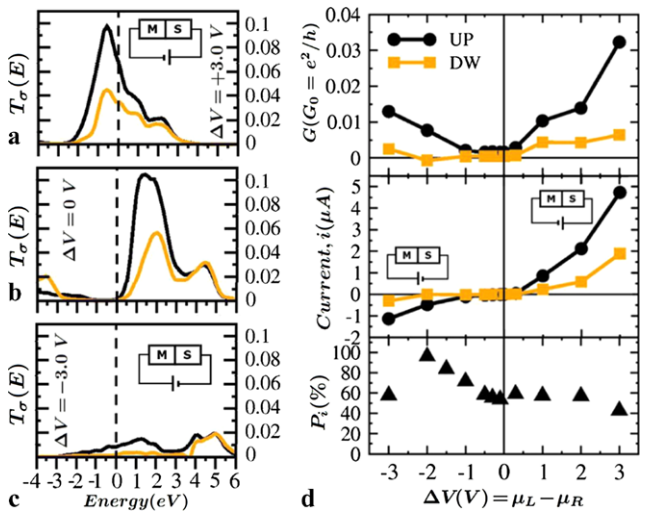

Fig. 4 (**a**–**c**) Spin-resolved transmission coefficients for different biases: $\Delta V = +3.0$ V, $\Delta V = 0$ V, and $\Delta V = -3.0$ V. (**d**) Spin-resolved conductance and current, and current spin-polarization ($P_i(\%) = \frac{i^{\uparrow} - i^{\downarrow}}{i^{\uparrow} + i^{\downarrow}} \times 100$) as a function of the applied bias voltage

electrochemical potential $\mu_L = 0$) and Fermi energy of the GeSe electrode is shifted by $\mu_R = -3.0$ eV, $\mu_R = 0$ eV, and $\mu_R = +3.0$ eV, corresponding to the three bias voltages $\Delta V = +3.0$ V, 0 V and -3.0 V ($\Delta V = \mu_L - \mu_R$) of the I–V curve shown in the middle panel of Fig. 4d. Details on the formalism behind this shifts can be found in [16], also the literature presents many examples of its application, e.g., [27–30]. Figure 4d shows the spin-resolved conductance and current, and the current spin-polarization. The current is calculated with the Landauer formula:

$$I_\sigma = \frac{e}{h} \int dE T_\sigma(E) \Delta f_{RL}(E) \tag{1}$$

where $\sigma = \text{UP, DW}$, $\Delta f_{RL}(E)$ is the difference of Fermi–Dirac distribution functions centered at the electrodes' electrochemical potentials, and the transmission $T_\sigma(E)$ is a k-space integrated expression within a Green's functions formalism [16]. The gap ($\sim$1 eV) of the GeSe electrode (away from the interface) implies the need of electrons to tunnel toward the metal for negative biases ($\Delta V < 0$). On the other hand, for direct bias electrons need not tunnel to go from the metal to the semiconductor conduction band, therefore, transmissions are higher for positive bias and the currents (both UP and DW, Fig. 4d, second panel) grow without a direct polarization gap (as the one observed in pn-junction diodes). The I–V curves clearly show that the heterojunction has a rectifying effect, especially for the DW-channel. In fact, the current spin polarization for negative bias shows a steep growth up to as high as $\sim$96 % for $\Delta V = -2.0$ V that quickly falls to $\sim$60 % for $\Delta V = -3.0$ V.

4 Conclusions

In this work, we assessed ground-state magnetoelectronic properties of the interface Cobalt/GeSe showing that the magnetic moment only penetrates about two atomic layers into the semiconductor and that both materials couple ferromagnetically. However, our calculations predict a spin-resolved current injection under bias voltage, indicating that the interface (i) has a spin dependent rectifying behavior (i.e., spin filter functionality), and (ii) yields current spin polarizations between $\sim$40 % and $\sim$96 %, features that suggest it is suitable for spintronic devices, making experimental studies upon this interface desirable.

Acknowledgements The authors acknowledge financial support from the Consejo Nacional de Investigaciones Científicas y Técnicas (CONICET) and the Universidad Nacional de Entre Ríos (UNER), Argentina; and the work of the developers of Xcrysden [31] and VESTA [32] codes, utilized in this work.

References

1. M.N. Baibich, J.M. Broto, A. Fert, F. Nguyen van Dau, F. Petroff, P. Etienne, G. Creuzet, A. Friederich, J. Chazelas, Phys. Rev. Lett. **61**, 2472 (1988)
2. R.Y. Yuan, R.Z. Wang, K. Xue, J.S. Wei, X.M. Song, B. Wang, H. Yan, Phys. Rev. B **74**, 024417 (2006)
3. P. Yordanov, A.V. Boris, J.W. Freeland, J.J. Kavich, J. Chakhalian, H.N. Lee, B. Keimer, Phys. Rev. B **84**, 045108 (2011)
4. A.G. Petukhov, D.O. Demchenko, A.N. Chantis, Phys. Rev. B **68**, 125332 (2003)
5. H. Oka, K. Tao, S. Wedekind, G. Rodary, V.S. Stepanyuk, D. Sander, J. Kirschner, Phys. Rev. Lett. **107**, 187201 (2011)
6. A.N. Useinov, J. Kosel, N.K. Useinov, L.R. Tagirov, Phys. Rev. B **84**, 085424 (2011)
7. R. Yamada, M. Noguchi, H. Tada, Appl. Phys. Lett. **98**, 053110 (2011)
8. I. Žutic, J. Fabian, S. Das Sarma, Rev. Mod. Phys. **76**, 323 (2004)
9. J.A.C. Bland, B. Heinrich (eds.), *Ultrathin Magnetic Structures IV* (Springer, Berlin, 2003)
10. G. Sun, R.A. Soref, H.H. Cheng, J. Appl. Phys. **108**, 033107 (2010)
11. K. Miyata, D.L. Dreifus, K. Kobashi, Appl. Phys. Lett. **60**(4), 480 (1992)
12. Y.-F. Qin, S.-S. Yan, S.-S. Kang, S.-Q. Xiao, Q. Li, Z.-Q. Dai, T.-T. Shen, Y.-Y. Dai, G.-L. Liu, Y.-X. Chen, L.-M. Mei, Z. Zhang, Chin. Phys. Lett. **28**(10), 107501 (2011)
13. Y.F. Tian, J.X. Deng, S.S. Yan, Y.Y. Dai, M.W. Zhao, Y.X. Chen, G.L. Liu, L.M. Mei, Z.Y. Liu, J.R. Sun, J. Appl. Phys. **107**, 024514 (2010)
14. B. Stärk, P. Krüger, J. Pollmann, Phys. Rev. B **81**, 035321 (2010)
15. T.T. Ong, A.M. Black-Schaffer, W. Shen, B.A. Jones, Phys. Rev. B **82**, 054429 (2010)
16. T. Ozaki, K. Nishio, H. Kino, Phys. Rev. B **81**, 035116 (2010)
17. T. Ozaki, Phys. Rev. B **67**, 155108 (2003)
18. T. Ozaki, H. Kino, Phys. Rev. B **69**, 195113 (2004)
19. J.P. Perdew, K. Burke, M. Ernzerhof, Phys. Rev. Lett. **77**, 3865 (1996)
20. J.P. Perdew, K. Burke, M. Ernzerhof, Generalized gradient approximation made simple. Phys. Rev. Lett. **78**, 1396 (1997)
21. J.P. Perdew, S. Kurth, A. Zupan, P. Blaha, Erratum: Accurate density functional with correct formal properties: a step beyond the generalized gradient approximation. Phys. Rev. Lett. **82**, 5179 (1999). [Phys. Rev. Lett. **82**, 2544 (1999)]
22. J. Chen, X. Wu, A. Selloni, Phys. Rev. B **83**, 245204 (2011)
23. A.B. Shick, O.N. Mryasov, Phys. Rev. B **67**, 172407 (2003)
24. A. Onodera, I. Sakamoto, Y. Fujii, N. Môri, S. Sugai, Phys. Rev. B **56**(13), 7935 (1997)
25. H.J. Monkhorst, J.D. Pack, Phys. Rev. B **13**, 5188 (1976)
26. L. Hongxia, Z. Heming, Z. Zhiyong, J. Semicond. **30**(5), 052002 (2009)
27. K. Nishio, T. Ozaki, T. Morishita, M. Mikami, Phys. Rev. B **81**, 115444 (2010)
28. T. Ozaki, K. Nishio, H. Weng, H. Kino, Phys. Rev. B **81**, 075422 (2010)
29. H. Jippo, M. Ohfuchi, C. Kaneta, Phys. Rev. B **84**, 075467 (2011)
30. M. Ohfuchi, T. Ozaki, C. Kaneta, Appl. Phys. Express **4**, 095101 (2011)
31. A. Kokalj, Comput. Mater. Sci. **28**, 155 (2003). Code available from http://www.xcrysden.org/
32. K. Momma, F. Izumi, J. Appl. Crystallogr. **44**, 1272 (2011)